



Anti-Corrosion Methods and Materials

Corrosion characterization of phosphated carbon steel treated with benzotriazole

Cristiane Spagnol Everson do Prado Banczek Isolda Costa Maico Taras Cunha André Lazarin Gallina Martha Tussolini Paulo Rogério Pinto Rodrigues

Article information:

To cite this document:

Cristiane Spagnol Everson do Prado Banczek Isolda Costa Maico Taras Cunha André Lazarin Gallina Martha Tussolini Paulo Rogério Pinto Rodrigues , (2015), "Corrosion characterization of phosphated carbon steel treated with benzotriazole", *Anti-Corrosion Methods and Materials*, Vol. 62 Iss 6 pp. 379 - 387

Permanent link to this document:

<http://dx.doi.org/10.1108/ACMM-07-2011-1137>

Downloaded on: 14 December 2015, At: 03:46 (PT)

References: this document contains references to 34 other documents.

To copy this document: permissions@emeraldinsight.com

The fulltext of this document has been downloaded 44 times since 2015*

Users who downloaded this article also downloaded:

Lin Liu, Xiaona Pan, Jinjuan Xing, Jianhua Qian, (2015), "Anti-corrosion behavior of thiadiazole derivatives for silver strip in hydrogen sulfide solutions", *Anti-Corrosion Methods and Materials*, Vol. 62 Iss 6 pp. 353-362 <http://dx.doi.org/10.1108/ACMM-03-2014-1364>

Yujie Zhang, Amir Poursaee, (2015), "Study of the semi-conductive behavior of the passive film on carbon steel in simulated concrete pore solution under stress", *Anti-Corrosion Methods and Materials*, Vol. 62 Iss 6 pp. 363-370 <http://dx.doi.org/10.1108/ACMM-04-2014-1375>

Tomasz Pawel Dudziak, Hailiang Du, Prasanta Datta, (2015), "Long exposure test in air, conducted on super-lattice coatings at 850°C for 4,000 hours", *Anti-Corrosion Methods and Materials*, Vol. 62 Iss 6 pp. 394-399 <http://dx.doi.org/10.1108/ACMM-03-2014-1366>

Access to this document was granted through an Emerald subscription provided by emerald-srm:478531 []

For Authors

If you would like to write for this, or any other Emerald publication, then please use our Emerald for Authors service information about how to choose which publication to write for and submission guidelines are available for all. Please visit www.emeraldinsight.com/authors for more information.

About Emerald www.emeraldinsight.com

Emerald is a global publisher linking research and practice to the benefit of society. The company manages a portfolio of more than 290 journals and over 2,350 books and book series volumes, as well as providing an extensive range of online products and additional customer resources and services.

Emerald is both COUNTER 4 and TRANSFER compliant. The organization is a partner of the Committee on Publication Ethics (COPE) and also works with Portico and the LOCKSS initiative for digital archive preservation.

*Related content and download information correct at time of download.

Corrosion characterization of phosphated carbon steel treated with benzotriazole

Cristiane Spagnol and Everson do Prado Banczek

Departamento de Química, Universidade Estadual do Centro-Oeste, Guarapuava, Brazil

Isolda Costa

Centro de Ciência e Tecnologia de Materiais, Instituto de Pesquisas Energéticas e Nucleares, IPEN/CNEN-SP, São Paulo, Brazil, and

Maico Taras Cunha, André Lazarin Gallina, Martha Tussolini and Paulo Rogério Pinto Rodrigues
Departamento de Química, Universidade Estadual do Centro-Oeste, Guarapuava, Brazil

Abstract

Purpose – The purpose of the paper is to show the corrosion effect of benzotriazole in comparison with iron phosphate (PFe) coating as a sealer for the PFe layer in carbon steel paint pre-treatment and to show its ecological advantages as a more environment-friendly inhibiting compound than PFe.

Design/methodology/approach – Samples of carbon steel (SAE 1010) were phosphated in two baths, one containing iron PFe and PFe and BTAH (PFe + BTAH). Anodic potentiostatic polarization curves and electrochemical impedance spectroscopy were used to evaluate the corrosion resistance of phosphated carbon steel in $0.1 \text{ mol L}^{-1} \text{ H}_2\text{SO}_4$, $0.5 \text{ mol L}^{-1} \text{ NaCl}$ and $0.1 \text{ mol L}^{-1} \text{ NaOH}$. The phosphate layers obtained were analyzed by infrared spectroscopy. Surface observation by scanning electron microscopy (SEM) showed that the PFe and PFe + BTAH layers are deposited as crystals with granular morphology. The electrochemical results showed that the PFe + BTAH coating was more effective in corrosion protection of the carbon steel.

Findings – This paper presents the application of benzotriazole as post-treatment of PFe-coated carbon steel. The results show that benzotriazole improves the phosphate layer properties. The SEM micrographs showed that the layer formed in PFe and PFe + BTAH baths consists of grain-like crystals, and infrared results revealed the BTAH presence in PFe phosphate. The corrosion resistance results showed higher efficiency associated to the PFe + BTAH phosphate layer relative to that of PFe. From the present study, results can be concluded that BTAH can be used as a post-treatment for PFe phosphate coating.

Originality/value – This paper deals with the corrosion resistance and surface carbon steel characterization of a new sealer for PFe coating, which has been prepared for this study and was never tested previously. These are candidate materials for substitution of chromium sealer. The BTAH sealer presents environmental and corrosion resistance advantages when compared with the post-treatment based on chrome. Although BTAH improves PFe layers' properties, it is the worst phosphate coating. This manuscript has never been previously submitted and deals with original results.

Keywords Corrosion, Benzotriazole, Carbon steel (SAE 1010), Iron phosphating, Phosphating

Paper type Research paper

1. Introduction

Phosphating is one of the most used surface treatments for metals (Banczek *et al.*, 2006; Jegannathan *et al.*, 2006a, 2006b; Wang *et al.*, 2006; Rout *et al.*, 2006; Jegannathan *et al.*, 2006a, 2006b; Rebeyrat *et al.*, 2002; Olesen *et al.*, 1998; Niu *et al.*, 2006; Whitten *et al.*, 2000; Bustamente *et al.*, 2003). It is known as a conversion coating that leads to the formation of insoluble phosphate salts and is used in many industries for corrosion protection, surface preparation or for decoration (Lorin, 1974).

This type of coating can be applied on steels (Banczek *et al.*, 2006; Jegannathan *et al.*, 2006a, 2006b; Wang *et al.*, 2006; Rout *et al.*, 2006; Olesen *et al.*, 1998), galvanized steel (Rout *et al.*, 2006; Bustamente *et al.*, 2003), iron (Rebeyrat *et al.*, 2002), magnesium (Niu *et al.*, 2006; Lian *et al.*, 2006), aluminium (Akhtar *et al.*, 2004) and zinc (Jegannathan *et al.*, 2005). There are many types of phosphating baths, such as iron (Lorin, 1974), zinc (Banczek *et al.*, 2006; Jegannathan *et al.*, 2005), manganese (Rout *et al.*, 2006; Weng *et al.*, 1997), tricationic (Banczek *et al.*, 2005) and organic phosphate (Rebeyrat *et al.*, 2002; Gang *et al.*, 1997).

Various types of chemical accelerators or additives for phosphating can be used, such as sodium nitrite (Banczek *et al.*,

The current issue and full text archive of this journal is available on Emerald Insight at: www.emeraldinsight.com/0003-5599.htm



Anti-Corrosion Methods and Materials
62/6 (2015) 379–387
© Emerald Group Publishing Limited [ISSN 0003-5599]
[DOI 10.1108/ACMM-07-2011-1137]

Authors are grateful to CAPES and CNPq for the financial support provided to this research.

Received 16 July 2011
Revised 15 December 2011
26 July 2012
13 November 2014
Accepted 10 July 2015

2006; Olesen *et al.*, 1998], nitrates (Wang *et al.*, 2006; Olesen *et al.*, 1998; Niu *et al.*, 2006; Lian *et al.*, 2006), chlorates (Górecki, 1995), calcium ions (Olesen *et al.*, 1998; Górecki, 1995), manganese ions (Weng *et al.*, 1997), tartaric acid (Niu *et al.*, 2006; Lian *et al.*, 2006), fluoride ions (Niu *et al.*, 2006; Akhtar *et al.*, 2004), nickel ions (Banczek *et al.*, 2006; Akhtar *et al.*, 2004; Górecki, 1995), copper ions (Blum and Kurt, 1975), molybdenum ions (Lian *et al.*, 2006), benzotriazole (Banczek *et al.*, 2006) and toltriazole (Banczek *et al.*, 2005).

Physically, the phosphate layer is not homogeneous. This heterogeneities cause cracks and porosities that reduce the corrosion resistance (Lorin, 1974). Post-phosphating process such as paint application can seal the areas where the substrate is exposed, improving the corrosion resistance. Sealing baths usually are at pH ranging between 2.0 and 4.8 (Górecki, 2000).

Hexavalent chromium in its oxide form (Lorin, 1974) is the most important sealer used after the phosphating process to improve the corrosion resistance of the metals, as the exposed areas become protected (Lorin, 1974). However, the toxicity of hexavalent chromium requires the development of new solutions (Sieg and Chattha, 1987).

Chromium in its oxidation form (+3), molybdate ions (Sieg and Chattha, 1987), epoxy resin (Sieg and Chattha, 1987), diphenylamine (Sieg and Chattha, 1987), solutions with aluminum and zirconium (Lindert, 1984) polyvinylphenol (Claffey and Reid, 1985) and titanium chelate (American Society for Testing Materials, 1983) are some examples of alternative sealers. Nevertheless, only a few of these promote the equivalent corrosion resistance (Sieg and Chattha, 1987). The aim of the present work was to study the action of BTAH as a bath after phosphating carbon steel (SAE 1010) with iron phosphate (PFe).

2. Experimental

2.1 Sample preparation

The material used as the substrate was carbon steel (SAE 1010) with a composition as shown in Table I.

Samples were prepared by SiC grinding in the sequence #220, #320, #400 and #600 grit. After grinding, the samples were degreased in a 5 per cent m/m alkaline solution for 5 min at $(70 \pm 5)^\circ\text{C}$ and then rinsed. Subsequently, the samples were immersed in an alkaline titanium phosphate salt solution with a concentration of 3 g/L (pH = 8), for 90 s at $(25 \pm 2)^\circ\text{C}$ for surface activation. Next, some samples were immersed in the phosphating bath, either with PFe only or with a post-phosphating solution containing $1 \times 10^{-3} \text{ molL}^{-1}$ BTAH which contained the PFe + BTAH coating, for 3 min at $(55 \pm 2)^\circ\text{C}$. In either case, after treatment, the samples were removed from the baths and dried in preparation for the evaluation tests.

2.2 Characterization of the phosphate layers

Phosphate layer morphology was evaluated using scanning electron microscopy (SEM). Energy dispersive spectroscopy

(EDS) spectra were used to determine the composition of the phosphate layers.

Infrared spectra were obtained using a Hartmann and Braun model FTIR BOMEM MB-100 spectrophotometer. Twenty-four scans were accomplished with a resolution of 4 cm^{-1} and carbon steel was used as the background.

Electrochemical behavior was evaluated from anodic potentiostatic polarization measurements and electrochemical impedance spectroscopy (EIS), using a frequency response analyzer (Gamry model EIS 300) coupled to a potentiostat type PCI4/300. Working electrodes with an area of 1.9 cm^2 were used in the electrochemical tests. A platinum wire and an Hg/Hg₂SO₄, Ag/AgCl and Hg/HgO electrode were used as counter and reference electrodes, respectively. Sulfuric acid solution (0.1 molL^{-1}), sodium chloride solution (0.5 molL^{-1}) and sodium hydroxide (0.1 molL^{-1}) were used for electrochemical characterization at $(20 \pm 2)^\circ\text{C}$.

Potentiostatic polarization tests were carried out from the corrosion potential E_{corr} up to an overpotential of +200 mV.

EIS measurements were performed potentiostatically at E_{corr} , with a perturbation of $\pm 5 \text{ mV}$ over the frequency range 100 kHz to 10 mHz, using an acquisition rate of 10 points per decade.

2.3 Accelerated corrosion and paint adherence

Salt spray (fog) testing was carried out in an Equilam model SSE500 fog chamber. Samples with a geometric area of 175 cm^2 were painted with a white electrostatic polyester powder. The procedure for carrying out the measurements is described by ASTM Standard B117 (American Society For Testing Materials, 1983). For coating adhesion testing, the ABNT Standard 11,003/1990 was used (Associação Brasileira de Normas Técnicas, 1990). Two cuts in X form were made in the organic film through to the metallic substrate using a knife.

3. Results

3.1 Morphology characterization of the phosphate layers

The layer morphology of the phosphate coating is shown in Figure 1. The PFe bath led to phosphate deposition on only few areas of the metallic substrate, as shown in Figure 1B.

Semi-quantitative elemental analyses obtained from the PFe and PFe + BTAH coatings using EDS are shown in Figures 2 and 3. The results show that the phosphate layer was formed on the carbon steel surface because both phosphorus and iron peaks are present in the spectrum.

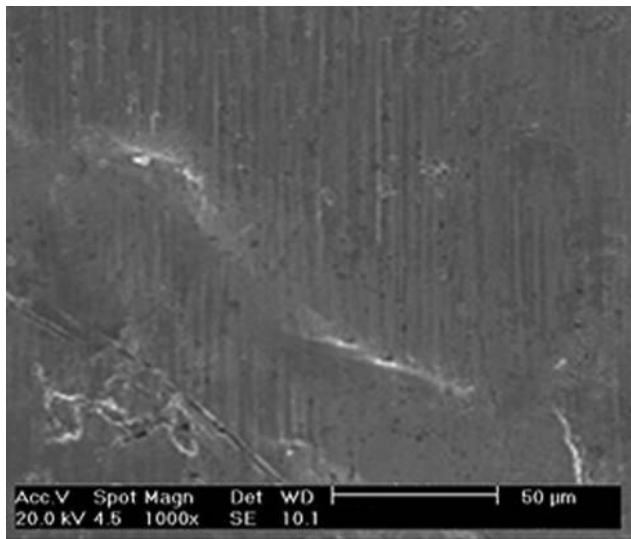
3.2 Infrared characterization

Infrared characterizations are shown in Figure 4. The IR spectra in Figure 4(A and B) correspond to the phosphate conversion layer. These results confirm the presence of PFe coating on the carbon steel surfaces that shows similar characteristic bands of phosphate on all of the obtained spectra.

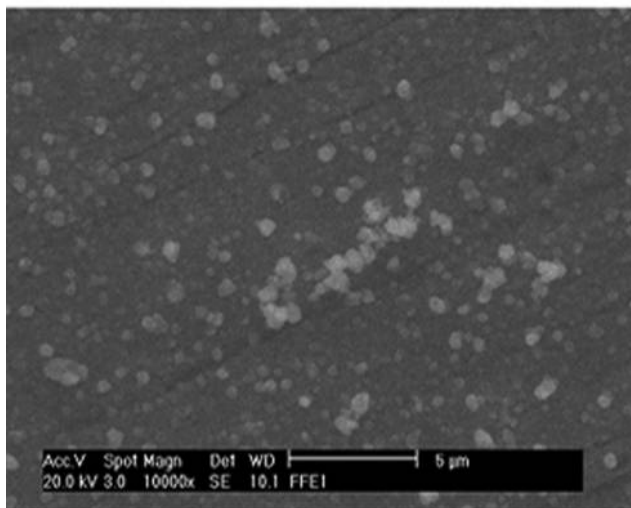
Table I Chemical composition of carbon steel (SAE 1010) used as substrate for phosphating

Carbon steel	C	Si	Mn	P	S	Cr	Ni	Mo
Elemental (%m/m)	0.118	0.023	0.310	0.020	0.016	0.024	0.028	0.002

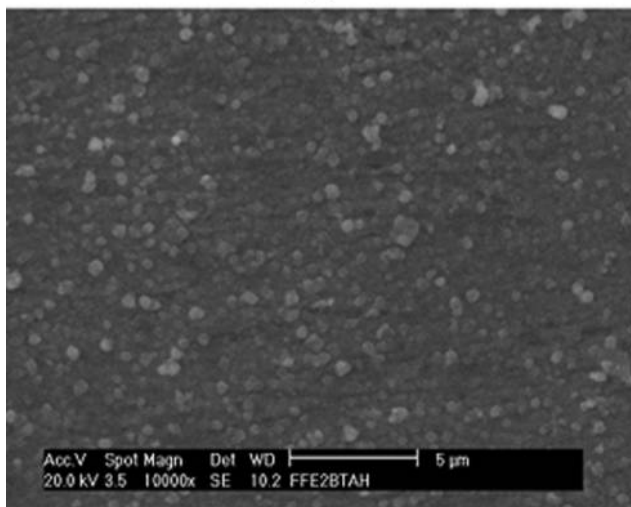
Figure 1 Scanning electron micrographs of (a) carbon steel (SAE 1010) and phosphate layer obtained (b) in PFe and (c) in PFe + BTAH



(a)

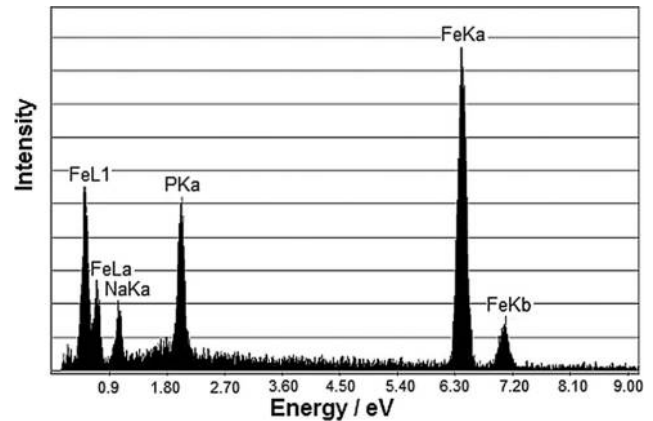


(b)

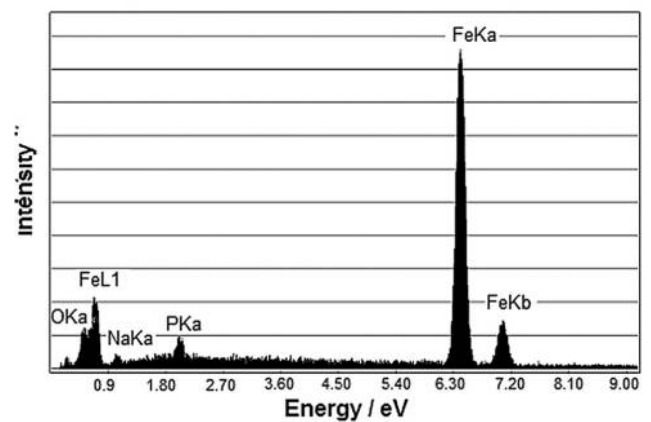


(c)

Figure 2 EDS spectra of the iron phosphated (PFe) carbon steel (SAE 1010) (a) white areas and (b) dark areas



(a)



(b)

3.3 Electrochemical characterization

3.3.1 In acid solution

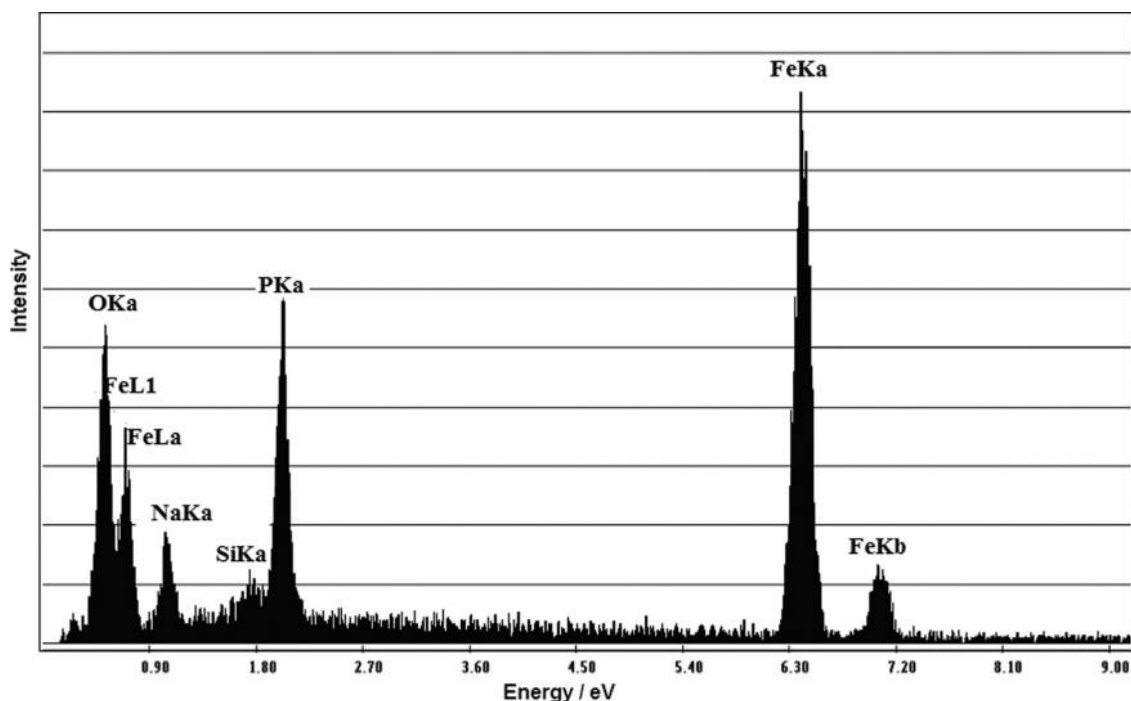
Anodic polarization curves obtained in $0.1 \text{ molL}^{-1} \text{ H}_2\text{SO}_4$ solution are shown in Figure 5. The EIS results obtained in $0.1 \text{ molL}^{-1} \text{ H}_2\text{SO}_4$ solution are shown in Figure 6. The results show active behavior for carbon steel-coated phosphate samples.

3.3.2 In neutral solution

The anodic potentiostatic polarization curves obtained in $0.5 \text{ molL}^{-1} \text{ NaCl}$ solution are shown in Figure 7. The EIS results obtained in $\text{NaCl } 0.5 \text{ molL}^{-1}$ solution are shown in Figure 8. A typical passive behavior is indicated for the PFe-phosphated samples at potentials close to E_{corr} in neutral media.

3.3.3 In alkaline solution

Anodic polarization curves obtained in $0.1 \text{ molL}^{-1} \text{ NaOH}$ solution are shown in Figure 9. Nyquist phase angle and Bode diagrams for the various tested samples in $0.1 \text{ molL}^{-1} \text{ NaOH}$ electrolyte are shown in Figure 10. A typical passive behavior is indicated for the unphosphated and PFe-phosphated samples at potentials close to E_{corr} , but the breakdown of this layer occurs at more positive potentials than for sodium chloride.

Figure 3 EDS spectra of the iron phosphated (PFe) carbon steel (SAE 1010) and treated with BTAH solution (PFe + BTAH)

3.4 Accelerated corrosion and paint adherence

Steel samples treated with PFe and PFe + BTAH phosphate were painted with organic paint. After exposure in the accelerated salt spray/fog cabinets, the phosphated samples were subjected to the paint adhesion tests. Sample shapes after 500 h are shown in Figures 11 and 12. The results show that the BTAH-passivated PFe layer showed higher corrosion resistance and greater paint adhesion.

4. Discussion

4.1 Morphology characterization of the phosphate layers

The phosphate layers formed in the PFe and PFe + BTAH phosphating baths [Figure 1(B and C)] both exhibited crystalline grains. Semi-quantitative elemental analyses obtained from the EDS on the PFe and PFe + BTAH coatings are shown in Figures 2 and 3. The EDS spectra of the white areas [Figure 2(A)] show the presence of the elements P and Fe that can be attributed the PFe layer. The dark area is the metallic substrate, because the EDS spectrum [Figure 2(B)] shows only an iron peak in large amounts. This element is mainly constituent of carbon steel.

4.2 Infrared characterization

In Figure 4(A), the bands close to 1037 cm^{-1} are typical P-O bond vibration (Rout *et al.*, 2006), at $2300\text{--}2450\text{ cm}^{-1}$ due to P-H bond stretching and at $950\text{--}1050\text{ cm}^{-1}$ due to P=O bond stretching (Barbosa, 2007). The iron phosphate FePO_4 band close to 900 and 1200 cm^{-1} are attributable to the vibrations of P-O and PO_4^{3-} bonds (He *et al.*, 2009).

Figure 4(B) shows that PFe + BTAH has the same behavior as the PFe coating, because the IR spectrum shows the same bands close to 1036 cm^{-1} that are typical of P-O bond

vibration (Rout *et al.*, 2006) at $2300\text{--}2450\text{ cm}^{-1}$ for P-H bond stretching (Barbosa, 2007) and at $950\text{--}1050\text{ cm}^{-1}$ for P=O bond stretching (Barbosa, 2007). The band for the iron phosphate FePO_4 , which is close to 900 and 1200 cm^{-1} , is attributed to the vibrations of P-O and PO_4^{3-} bonds (He *et al.*, 2009).

The presence of BTAH in the PFe coating can be observed through comparison between Figure 4(B and C). The N-H functional group in BTAH shows a band close to 3465 cm^{-1} (Ravichandran *et al.*, 2004). The C-H aromatic bond shows a less intense peak between 2900 and 3300 cm^{-1} and bands close to $1500\text{--}1600\text{ cm}^{-1}$ were shown for N-H (Selvi *et al.*, 2003).

The two peaks after 900 cm^{-1} might indicate the presence of BTAH in PFe + BTAH coating and the presence of N-H bands close to 1215 and 1100 cm^{-1} also was indicative of this compound (Rodrigues, 1997).

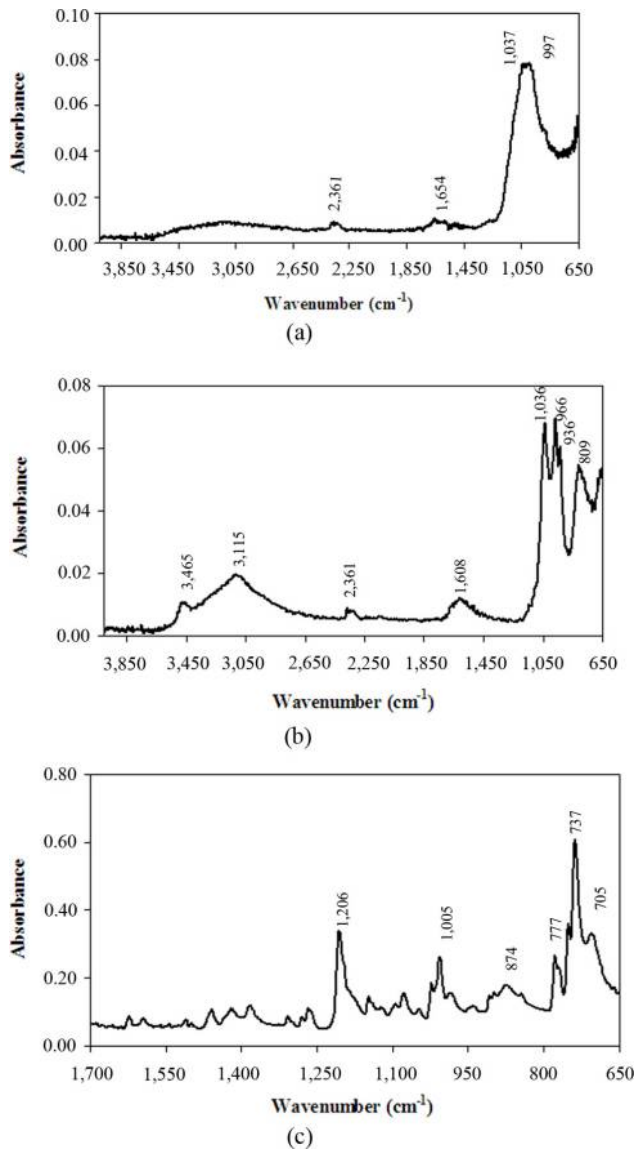
4.3 Electrochemical characterization

4.3.1 In acid solution

Typical anodic polarization curves obtained in 0.1 molL^{-1} H_2SO_4 solution are shown in Figure 5. The current densities for the phosphated samples were lower than those for the carbon steel. However, all of the samples presented high current densities, typical of active dissolution, showing that the phosphate layer did not cause surface passivation in the acid medium.

The inherent porosity of the phosphate layer allows free access of acid to the carbon steel substrate causing the detachment of the phosphate layer. This is a shortcoming of phosphate coatings for the corrosion protection of the metal in such environments (Banczek *et al.*, 2006; Weng *et al.*, 1997). However, smaller current densities were measured

Figure 4 Infrared spectrum of the phosphate carbon steel phosphated in (a) PFe, (b) PFe and treated with BTAH solution (PFe + BTAH) and (c) BTAH powder



for the PFe + BTAH covered samples. This result suggests that the more uniform structure of the phosphate coating, together perhaps with impregnation of the coating with BTAH, improves the corrosion protection of the carbon steel to some slight extent.

Nyquist diagrams (Figure 6) feature a single capacitive semicircle suggesting activation control and only one time constant, which is typical of acidic corrosion of carbon steel. This was also supported by the Bode diagrams that showed only a phase angle peak at frequencies around 100 Hz. Data obtained for the phosphated samples at low frequencies indicated an inductive behavior for all samples in the acid electrolyte. This has been related in literature to iron dissolution (Banczek *et al.*, 2006; Epelboin *et al.*, 1979), due to the substrate attack, also supporting the poor protection afforded by the phosphate layer in the acidic media.

Figure 5 Anodic potentiostatic polarization curves obtained in $0.1 \text{ molL}^{-1} \text{ H}_2\text{SO}_4$ solution for the carbon steel (SAE 1010) unphosphated or phosphate in PFe or PFe + BTAH

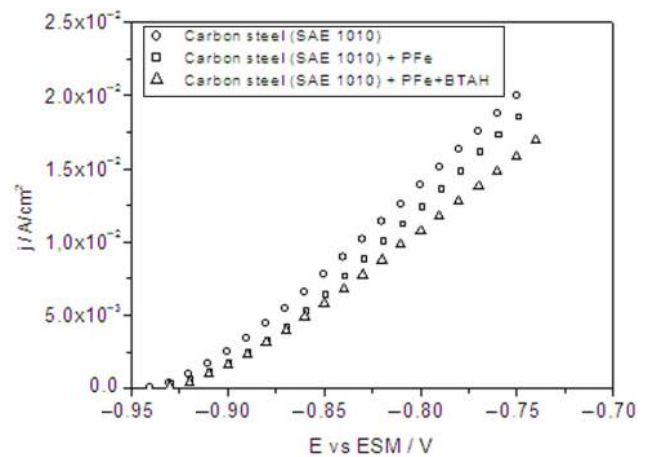
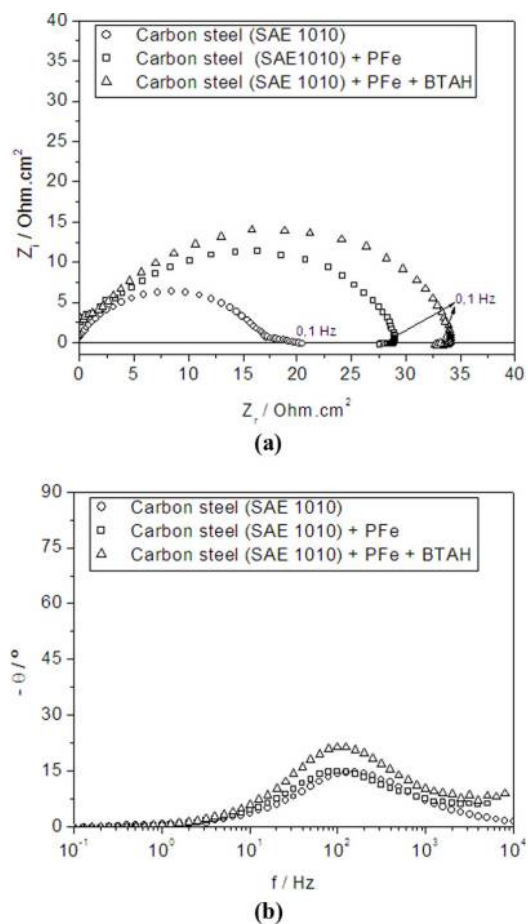


Figure 6 Nyquist and Bode phase angle diagrams obtained after immersion in $0.1 \text{ molL}^{-1} \text{ H}_2\text{SO}_4$ solution, for unphosphated or phosphated carbon steel in PFe or PFe + BTAH



4.3.2 In neutral solution

Figure 7 shows the anodic potentiostatic polarization curves obtained in $0.5 \text{ molL}^{-1} \text{ NaCl}$ solution. A typical passive behavior is indicated for the PFe-phosphated samples at

Figure 7 Anodic potentiostatic polarization curves obtained in 0.5 molL^{-1} NaCl solution for the carbon steel (SAE 1010) unphosphated or phosphate in PFe or PFe + BTAH

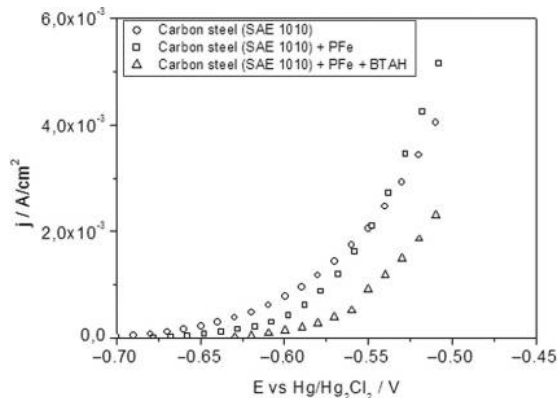
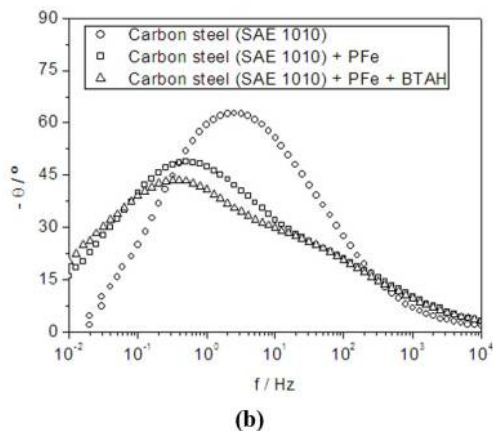
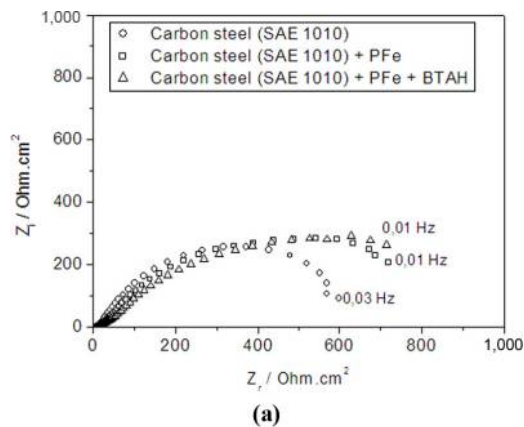
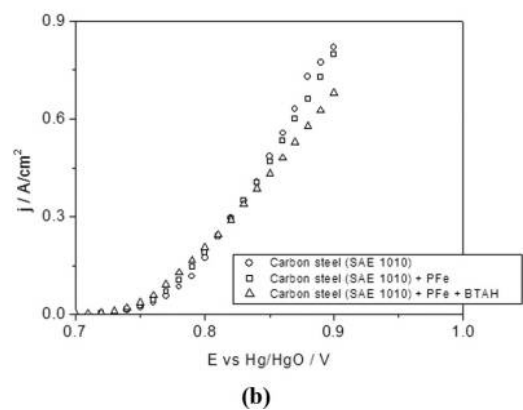
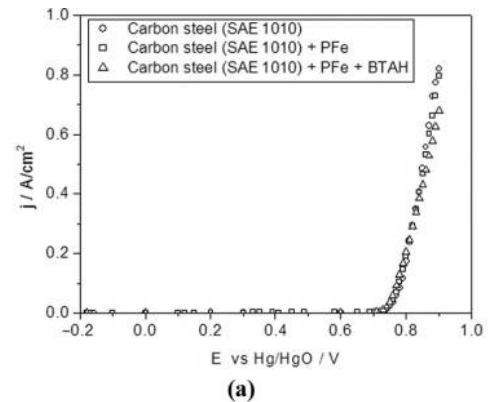


Figure 8 Nyquist and Bode phase angle diagrams obtained after immersion in 0.5 molL^{-1} NaCl solution, for unphosphated or phosphated carbon steel in PFe or PFe + BTAH



potentials close to E_{corr} , but breakdown of this layer occurs at potentials of approximately -600 and -550 mV, respectively, for samples phosphated in PFe and PFe + BTAH baths. These results indicate the better resistance of PFe + BTAH coating layer compared with that of the PFe. EIS results obtained in NaCl 0.5 molL^{-1} solution are shown in Figure 8. For the carbon steel, only a single time constant is indicated. A phase angle peak is seen on the Bode diagram

Figure 9 Anodic potentiostatic Polarization curves obtained in 0.1 molL^{-1} NaOH solution for the carbon steel (SAE 1010) unphosphated or phosphate in PFe or PFe + BTAH



at approximately 1 Hz, with a time constant that is associated with the charge transfer reaction. Nyquist diagrams for the phosphated steel samples show one capacitive arc suggesting one time constant, whereas the Bode diagrams indicate two time constants. The first time constant is shown at higher frequencies (1000 Hz) for the phosphated samples and is associated with pore resistance to electrolyte penetration. Phase angles at the high frequencies were the same for all of the phosphate layers, suggesting the same behavior.

The phase angle peak at 0.1 Hz for the phosphated samples was attributed to the substrate/electrolyte interface interaction underneath the phosphate layer (Banczek *et al.*, 2006). The phase angle peak in 0.1 Hz for PFe + BTAH moved to lower frequencies, which indicates the marginally better corrosion protection properties associated with this coating.

4.3.3 In alkaline solution

Anodic polarization curves obtained in 0.1 molL^{-1} NaOH solution are shown in Figure 9. Typical passive behavior is indicated for the unphosphated and PFe-phosphated samples at potentials close to E_{corr} , but breakdown of this layer occurs at potentials of approximately 800 mV. These results indicate a similar behavior by both types of sample. This behavior could be related to the oxide/hydroxide layer formation. In alkaline solution, the phosphate coating is dissolved (Weng *et al.*, 1997) because Fe^{2+} is rusted to Fe^{3+} forming the oxide/hydroxide layer.

Figure 10 Nyquist and Bode phase angle diagrams obtained after immersion in 0.1 molL^{-1} NaOH solution, for unphosphated or phosphated carbon steel in PFe or PFe + BTAH

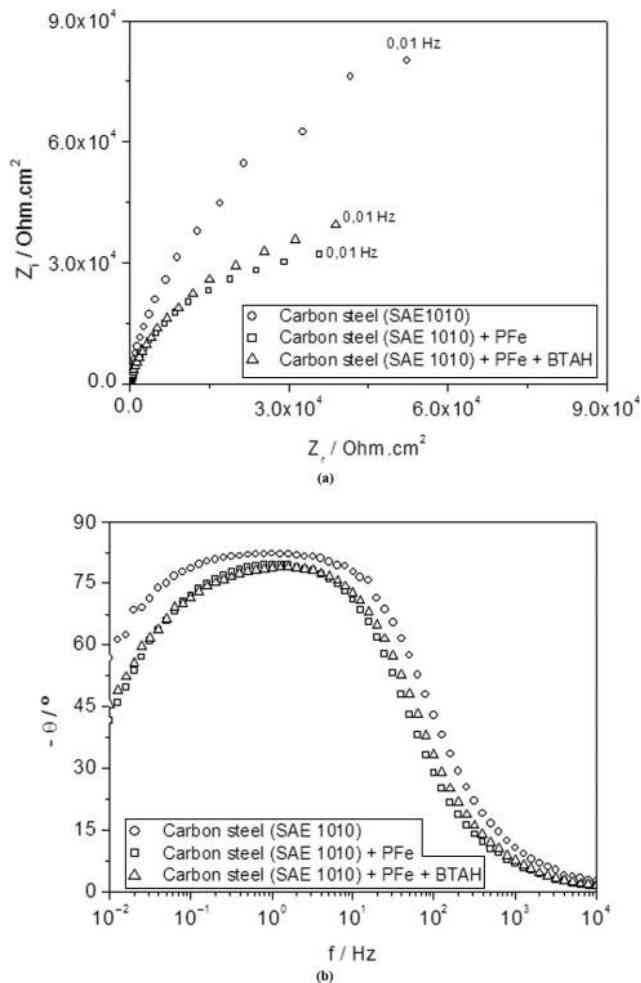


Figure 12 Corrosion test for painted samples after iron phosphating in (a) PFe/BTAH/Paint before test, (b) PFe/BTAH/Paint after test and (c) PFe/BTAH/Paint after adherence test

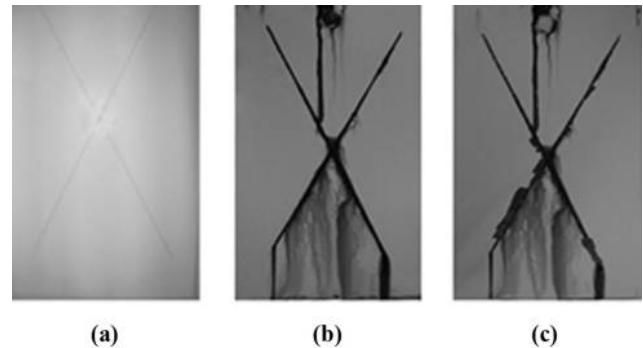
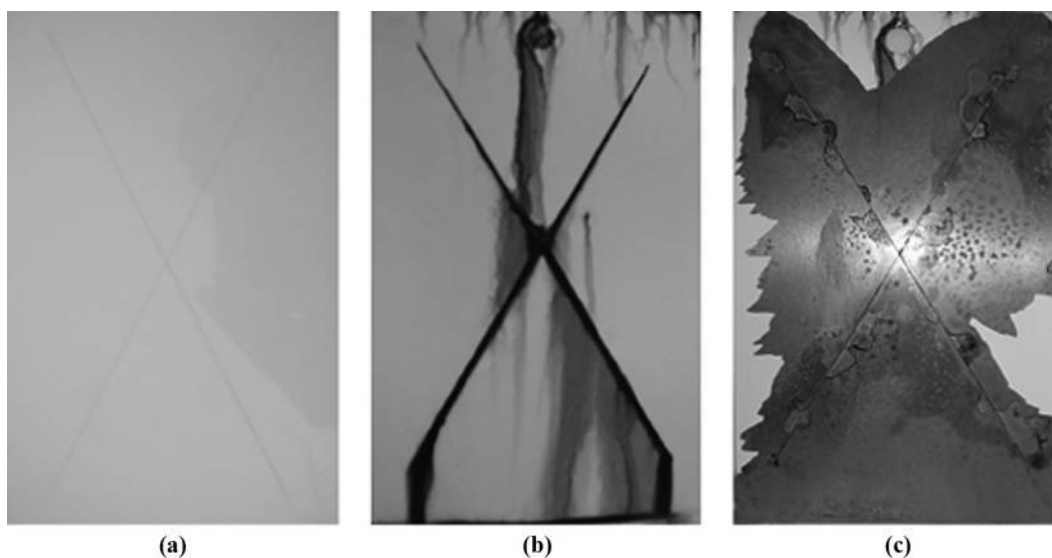


Figure 9(B) shows the anodic polarization curves in the active regions. The current densities were smaller for the PFe + BTAH-phosphated samples, and this result indicates better corrosion protection behavior.

Nyquist and Bode phase angle diagrams for the various tested samples in 0.1 molL^{-1} NaOH electrolyte are shown in Figure 10. The Nyquist diagrams for the phosphated samples show one flattened capacitive semicircle, and the Bode diagrams for the same samples show a large phase angle peak from 10 Hz until approximately 0.1 Hz, suggesting the interaction of more than one time constant. For the unphosphated substrate, the same behavior was obtained because of the iron oxide/hydroxide layer formation. The peak close to 10 Hz was associated with the pore resistance for electrolyte penetration into the iron oxide/hydroxide layer. The phase angle peak at 0.1 Hz for the unphosphated samples was attributed to the substrate/electrolyte interface interaction underneath the oxide/hydroxide layer.

The large peak at high frequencies and at phase angles lower than 80° is associated with pores in the phosphate layer. There are reports in the literature (Song et al., 2000) that for porous

Figure 11 Corrosion test for painted samples after iron phosphating in (a) PFe/Paint before test, (b) PFe/Paint after test and (c) PFe/Paint after adherence test



electrodes, the high frequency response depends on the AC signal penetrability into the pores. If the AC signal does not penetrate as deep as the pores' length, the response represents only the pore response and phase angles between 45° and 90° are obtained. The time constant at low frequencies is probably due to corrosive attack of the exposed substrate. The Nyquist diagrams showed that the phosphate coating had a smaller impedance value. This may be because the iron oxide/hydroxide layer formation degrades the phosphate coating.

4.3 Accelerated corrosion and paint adherence

In PFe phosphate coatings [Figure 11(B)], the corrosion rate was higher than for samples phosphated in the PFe + BTAH bath [Figure 12(B)]. From this, it can be concluded that coatings produced in the PFe + BTAH-phosphating solution afford higher corrosion protection, mainly due to the improved surface coverage.

After exposure in the salt spray cabinet, the paint adhesion tests were carried out, and the results presented in Figures 11(C) and 12(C) showed that the amount of paint removed was larger on PFe-coated samples than for samples prepared with PFe + BTAH coatings. It can be concluded that the phosphated samples with PFe + BTAH coatings gave higher paint adhesion. Comparing the images in Figures 11 and 12, samples with the PFe + BTAH coatings exhibited better corrosion resistance and paint adhesion than did those coated using the PFe treatment.

5. Conclusions

SEM micrographs showed that the phosphate layers formed in PFe and PFe + BTAH baths consisted of grain-like crystals. However, the morphology of the layer formed in the PFe + BTAH solution resulted in enhanced surface and IR results associated with the presence of BTAH in PFe-phosphated carbon steel surface.

Electrochemical characterization of the phosphate layers obtained showed better corrosion resistance and, consequently, higher efficiency associated to the phosphate layer deposited in the PFe + BTAH compared with that in the PFe. From the results of the present study, it can be concluded that BTAH can be used as a post-treatment for PFe phosphate coating.

References

- Akhtar, A.S., Susac, D., Glaze, P., Wong, K.C.K. and Mitchell, A.R. (2004), "The effect of Ni²⁺ on zinc phosphating of 2024-T3 Al alloy", *Surface and Coatings Technology*, Vol. 187 No. 3, pp. 208-215.
- American Society for Testing Materials (1983), *Standard Test Method of Salt Spray (Fog) Testing*, American Society for Testing Materials, Philadelphia, PA.
- Associação Brasileira de Normas Técnicas (1990), *Tintas – Determinação da aderência*, Associação Brasileira de Normas Técnicas, Rio de Janeiro.
- Banczek, E.P., Oliveira, M.F., Cunha, M.T. and Rodrigues, P.R.P. (2005), "Study of the electrochemical behaviour of toltriazole in phosphating baths for carbon steel 1008", *Portugaliae Electrochimica Acta*, Vol. 23 No. 3, pp. 379-391.
- Banczek, E.P., Rodrigues, P.R.P. and Costa, I. (2006), "Investigation on the effect of benzotriazole on the phosphating of carbon steel", *Surface and Coatings Technology*, Vol. 201 No. 6, pp. 3701-3708.
- Barbosa, L.C.A. (2007), *Espectroscopia no Infravermelho na Caracterização de Compostos Orgânicos*, Universidade Federal de Viçosa, Viçosa..
- Blum, W.A. and Kurt, G. (1975), "Scaling rinse for phosphate coatings of metal", US Patent 3. 895.970.
- Bustamente, G., Fabri, M.F.J.I., Margarit, C.P. and Mattos, O.R. (2003), "Influence of prephosphating on painted electrogalvanized steel", *Progress in Organic Coating*, Vol. 46 No. 2, pp. 84-90.
- Claffey, W.J. and Reid, A.J. (1985), "Post treatment of phosphated metal surfaces by organic titanates", US Patent 4. 656.097.
- Epelboin, I., Mattos, O.R., Keddani, M. and Takenouti, H. (1979), "The dissolution and passivation of Fe and Fe-Cr alloys in acidified sulphate medium: influences of pH and Cr content", *Corrosion Science*, Vol. 19 No. 7, pp. 1105-1112.
- Gang, L., Wangen, S., Yanrong, C. and Shili, Z. (1997), "Organic phosphating at room temperature", *Metal Finishing*, Vol. 95 No. 9, pp. 54-57.
- Górecki, G. (1995), "Improved iron phosphate corrosion resistance by modification with metal ions", *Metal Finishing*, Vol. 93 No. 3, pp. 36-39.
- Górecki, G. (2000), "Function of final (seal) rinses in a phosphating operation", *Metal Finishing*, Vol. 98 No. 8, pp. 100-101.
- He, W., Zhou, W., Wnag, Y., Zhang, X., Zhao, H., Li, Z. and Yan, S. (2009), "Biomaterialization of iron phosphate nanoparticles in yeast cells", *Materials Science and Engineering*, Vol. 29 No. 4, pp. 1348-1350.
- Jegannathan, S., Narayanan, T.S.N., Ravichandran, S.K. and Rajeswari, S. (2005), "Performance of zinc phosphate coatings obtained by cathodic electrochemical treatment in accelerated corrosion tests", *Electrochimica Acta*, Vol. 51 No. 2, pp. 247-256.
- Jegannathan, S., Narayanan, T.S.N.S., Ravichandran, K. and Rajeswari, S. (2006a), "Formation of zinc phosphate coating by anodic electrochemical treatment", *Surface and Coatings Technology*, Vol. 200 No. 21, pp. 6014-6021.
- Jegannathan, S., Sankara, N.T.S.N., Ravichandran, K. and Rajeswari, S. (2006b), "Formation of zinc-zinc phosphate composite coatings by cathodic electrochemical treatment", *Surface and Coatings Technology*, Vol. 200 No. 13, pp. 4117-4126.
- Lian, J.S., Li, G.Y., Niu, L.Y., Gu, C.D., Jiang, Z.H. and Jiang, Q. (2006), "Electroless Ni-P deposition plus zinc phosphate coating on AZ91D magnesium alloy", *Surface and Coatings Technology*, Vol. 200 No. 20, pp. 5956-5962.
- Lindert, A. (1984), "Process and solution for surface treatment of a metallic surface", BR PI Pat. 8402197.
- Lorin, G. (1974), *Phosphating of Metals*, Middlesex, Finishing Publications, Great Britain.
- Niu, L.Y., Jiang, Z.H., Li, G.Y., Gu, C.D. and Lian, J.S. (2006), "A study and application of zinc phosphate coating

- on AZ91D magnesium alloy”, *Surface and Coatings Technology*, Vol. 200 No. 9, pp. 3021–3026.
- Olesen, P.T., Steenberg, T., Christensen, E. and Bjerrum, N.J. (1998), “Electrolytic deposition of amorphous and crystalline zinc–calcium phosphates”, *Journal Materials Science*, Vol. 33 No. 12, pp. 3059–3063.
- Ravichandran, S., Najundan, R.S. and Rajendran, N. (2004), “Effect of benzotriazole derivatives on the corrosion of brass in NaCl solutions”, *Applied Surface Science*, Vol. 236 No. 4, pp. 241–250.
- Rebeyrat, S., Grosseau, P.J., Silvain, L.J.F., Panicaud, B. and Dinhut, J.F. (2002), “Phosphating of bulk α -iron and its oxidation resistance at 400°C”, *Applied Surface Science*, Vol. 199 No. 1, pp. 11–21.
- Rodrigues, P.R.P. (1997), “O Benzotriazol como inibidor de corrosão para ferro e ligas ferrosas em meios de ácido sulfúrico”, PhD thesis, Instituto de Química da Universidade de São Paulo, São Paulo.
- Rout, T.K., Pradhan, H.K. and Venugopalan, T. (2006), “Enhanced forming properties of galvanized steel sheet by polymanganese phosphate coating”, *Surface and Coatings Technology*, Vol. 201 No. 6, pp. 3496–3501.
- Selvi, S.T., Raman, V. and Rajendran, N. (2003), “Corrosion inhibition of mild steel by benzotriazole derivatives in acidic medium”, *Journal of Applied Electrochemistry*, Vol. 33 No. 12, pp. 1175–1182.
- Shenglin, Z., Xiaolin, Z. and Mingming, Z. (2008), “Zinc phosphating of 6061-A1 alloy using REN as additive”, *Journal of Rare Earths*, Vol. 26 No. 1, pp. 110–114.
- Sieg, W.O. and Chattha, M.S. (1987), “Corrosion inhibiting aqueous compositions comprising metal-chelating diphenolamine compounds”, US Patent 4. 790. 878.
- Song, H.K., Hwang, H.Y., Lee, K.H. and Dao, L.H. (2000), “The effect of pore size distribution on the frequency dispersion of porous electrodes”, *Electrochimica Acta*, Vol. 45 No. 14, pp. 2241–2257.
- Weng, D., Jokiel, P., Uebleis, A. and Boehni, H. (1997), “Corrosion and protection characteristics of zinc and manganese phosphate coatings”, *Surface and Coatings Technology*, Vol. 88 No. 3, pp. 147–156.
- Wang, C.M., Liao, H.C. and Tsai, W.T. (2006), “Effects of temperature and applied potential on the microstructure and electrochemical behavior of manganese phosphate coating”, *Surface and Coatings Technology*, Vol. 201 No. 6, pp. 2994–3001.
- Whitten, M.C. and Lin, C.T. (2000), “An in situ phosphating coating on 2024 T3 aluminum coupons”, *Progress in Organic Coating*, Vol. 38 No. 4, pp. 151–162.
- Wimmer, W., Gottschlich, J., Motorenwerke, B., Bush, E. and Gehmecker, H. (1998), “Nickel-and nitrite-free pretreatment of car bodies”, *Metal Finishing*, Vol. 38 No. 6, pp. 16–19.

Corresponding author

Everson do Prado Banczek can be contacted at: edopradobanczek@yahoo.com.br